2.6 Stress Analysis of Cracks

For certain cracked configurations subjected to external forces, it is possible to derive closed-form expressions for the stresses in the body, assuming isotropic linear elastic material behavior. Westergaard [8], Irwin [9], Sneddon [10], and Williams [11] were among the first to publish such solutions. If we define a polar coordinate axis with the origin at the crack tip (Figure 2.13), it can be shown that the stress field in any linear elastic cracked body is given by

$$\sigma_{ij} = \left(\frac{k}{\sqrt{r}}\right) f_{ij}(\theta) + \sum_{m=0}^{\infty} A_m r^{m/2} g_{ij}^{(m)}(\theta) \tag{2.41}$$

where σ_{ij} is the stress tensor; r and θ are as defined in Figure 2.13; k a constant; and f_{ij} is a dimensionless function of θ in the leading term. For the higher-order terms, A_m is the amplitude and $g_{ij}^{(m)}$ is a dimensionless function of θ for the mth term. The higher-order terms depend on the geometry, but the solution for any given configuration contains a leading term that is proportional to $1/\sqrt{r}$. As $r \to 0$, the leading term approaches infinity, but the other terms remain finite or approach zero. Thus stress near the crack tip varies with $1/\sqrt{r}$, regardless of the configuration of the cracked body. It can also be shown that the displacement near the crack tip varies with $\sqrt{r}$. Equation 2.41 describes a stress *singularity*, since stress is asymptotic to $r = 0$. The basis of this relationship is explored in more detail in Appendix 2A.3. Recall that the Inglis analysis (Section 2.2) predicts a stress singularity at the tip of a perfectly sharp crack.

There are three types of loading that a crack can experience, as Figure 2.14 illustrates. Mode I loading, where the principal load is applied normal to the crack plane, tends to open the crack. Mode II corresponds to in-plane shear loading and tends to slide one crack face with respect to the other. Mode III refers to out-of-plane shear. A cracked body can be loaded in any one of these modes, or a combination of two or three modes.

2.6.1 The Stress Intensity Factor

Each mode of loading produces the $1/\sqrt{r}$ singularity at the crack tip, but the proportionality constant, k, and f_{ij} depend on the mode. It is convenient at this point to replace k by

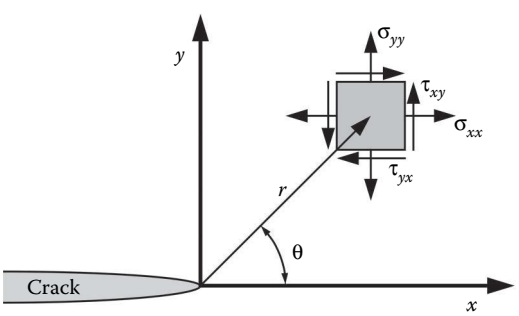

FIGURE 2.13
Definition of the coordinate axis ahead of a crack tip. The z direction is normal to the page.

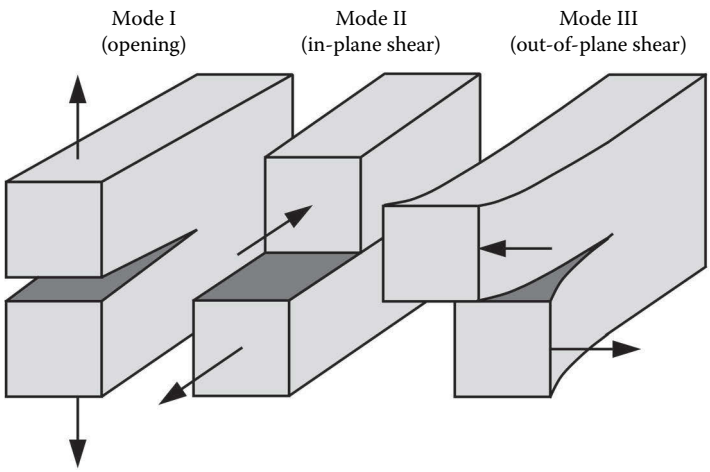

FIGURE 2.14
The three modes of loading that can be applied to a crack.

the *stress intensity factor*, K, where $K = k\sqrt{2\pi}$. The stress intensity factor is usually given a subscript to denote the mode of loading; that is, K_I, K_{II}, or K_{III}. Thus the stress fields ahead of a crack tip in an isotropic linear elastic material can be written as

$$\lim_{r\to 0} \sigma_{ij}^{(\mathrm{I})} = \frac{K_I}{\sqrt{2\pi r}} f_{ij}^{(\mathrm{I})}(\theta) \tag{2.42}$$

$$\lim_{r\to 0} \sigma_{ij}^{(\mathrm{II})} = \frac{K_{II}}{\sqrt{2\pi r}} f_{ij}^{(\mathrm{II})}(\theta) \tag{2.43}$$

$$\lim_{r\to 0} \sigma_{ij}^{(\mathrm{III})} = \frac{K_{III}}{\sqrt{2\pi r}} f_{ij}^{(\mathrm{III})}(\theta) \tag{2.44}$$

for Modes I, II, and III, respectively. In a mixed-mode problem (i.e., when more than one loading mode is present), the individual contributions to a given stress component are additive:

$$\sigma_{ij}^{(\text{total})} = \sigma_{ij}^{(\mathrm{I})} + \sigma_{ij}^{(\mathrm{II})} + \sigma_{ij}^{(\mathrm{III})} \tag{2.45}$$

Equation 2.45 stems from the principle of linear superposition.

Detailed expressions for the singular stress fields for Modes I and II are given in Table 2.1, where the stress tensors are expressed in Cartesian coordinates. Displacement relationships for Modes I and II are listed in Table 2.2. Table 2.3 lists the nonzero stress and displacement components for Mode III.

Consider the Mode I singular field on the crack plane, where $\theta = 0$. According to Table 2.1, the stresses in the x and y direction are equal:

$$\sigma_{xx} = \sigma_{yy} = \frac{K_I}{\sqrt{2\pi r}} \tag{2.46}$$

TABLE 2.1

Stress Fields Ahead of a Crack Tip for Modes I and II in a Linear Elastic, Isotropic Material

	Mode I	**Mode II**
σ_{xx}	$\frac{K_I}{\sqrt{2\pi r}}\cos\left(\frac{\theta}{2}\right)\left[1-\sin\left(\frac{\theta}{2}\right)\sin\left(\frac{3\theta}{2}\right)\right]$	$-\frac{K_{II}}{\sqrt{2\pi r}}\sin\left(\frac{\theta}{2}\right)\left[2+\cos\left(\frac{\theta}{2}\right)\cos\left(\frac{3\theta}{2}\right)\right]$
σ_{yy}	$\frac{K_I}{\sqrt{2\pi r}}\cos\left(\frac{\theta}{2}\right)\left[1+\sin\left(\frac{\theta}{2}\right)\sin\left(\frac{3\theta}{2}\right)\right]$	$\frac{K_{II}}{\sqrt{2\pi r}}\sin\left(\frac{\theta}{2}\right)\cos\left(\frac{\theta}{2}\right)\cos\left(\frac{3\theta}{2}\right)$
τ_{xy}	$\frac{K_I}{\sqrt{2\pi r}}\cos\left(\frac{\theta}{2}\right)\sin\left(\frac{\theta}{2}\right)\cos\left(\frac{3\theta}{2}\right)$	$\frac{K_{II}}{\sqrt{2\pi r}}\cos\left(\frac{\theta}{2}\right)\left[1-\sin\left(\frac{\theta}{2}\right)\sin\left(\frac{3\theta}{2}\right)\right]$
σ_{zz}	0 (Plane Stress) $\nu(\sigma_{xx}+\sigma_{yy})$ (Plane Strain)	0 (Plane Stress) $\nu(\sigma_{xx}+\sigma_{yy})$ (Plane Strain)
τ_{xz}, τ_{yz}	0	0

Note: ν is Poisson's ratio.

TABLE 2.2

Crack Tip Displacement Fields for Modes I and II (Linear Elastic, Isotropic Material)

	Mode I	**Mode II**
u_x	$\frac{K_I}{2\mu}\sqrt{\frac{r}{2\pi}}\cos\left(\frac{\theta}{2}\right)\left[\kappa-1+2\sin^2\left(\frac{\theta}{2}\right)\right]$	$\frac{K_{II}}{2\mu}\sqrt{\frac{r}{2\pi}}\sin\left(\frac{\theta}{2}\right)\left[\kappa+1+2\cos^2\left(\frac{\theta}{2}\right)\right]$
u_y	$\frac{K_I}{2\mu}\sqrt{\frac{r}{2\pi}}\sin\left(\frac{\theta}{2}\right)\left[\kappa+1-2\cos^2\left(\frac{\theta}{2}\right)\right]$	$-\frac{K_{II}}{2\mu}\sqrt{\frac{r}{2\pi}}\cos\left(\frac{\theta}{2}\right)\left[\kappa-1-2\sin^2\left(\frac{\theta}{2}\right)\right]$

Note: μ is the shear modulus; $\kappa = 3 - 4\nu$ (plane strain); $\kappa = (3-\nu)/(1+\nu)$ (plane stress).

When $\theta = 0$, the shear stress is zero, which means that the crack plane is a principal plane for pure Mode I loading. Figure 2.15 is a schematic plot of σ_{yy}, the stress normal to the crack plane, versus the distance from the crack tip. Equation 2.46 is valid only near the crack tip, where the $1/\sqrt{r}$ singularity dominates the stress field. Stresses far from the crack tip are governed by the remote boundary conditions. For example, if the cracked

TABLE 2.3

Nonzero Stress and Displacement Components in Mode III (Linear Elastic, Isotropic Material)

$$\tau_{xz} = -\frac{K_{III}}{\sqrt{2\pi r}}\sin\left(\frac{\theta}{2}\right)$$

$$\tau_{yz} = \frac{K_{III}}{\sqrt{2\pi r}}\cos\left(\frac{\theta}{2}\right)$$

$$u_z = \frac{2K_{III}}{\mu}\sqrt{\frac{r}{2\pi}}\sin\left(\frac{\theta}{2}\right)$$

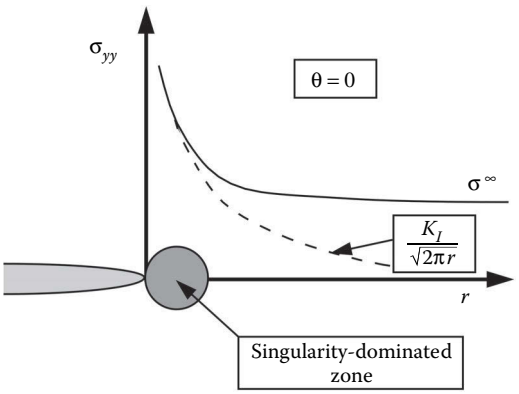

FIGURE 2.15
Stress normal to the crack plane in Mode I.

structure is subjected to a uniform remote tensile stress, σ_{yy} approaches a constant value, σ^{∞}. We can define a *singularity-dominated zone* as the region where the equations in Tables 2.1 through 2.3 describe the crack tip fields.

The stress intensity factor defines the amplitude of the crack tip singularity. That is, stresses near the crack tip increase in proportion to K. Moreover, the stress intensity factor completely defines the crack tip conditions; if K is known, it is possible to solve for all components of stress, strain, and displacement as a function of r and θ. This single-parameter description of crack tip conditions turns out to be one of the most important concepts in fracture mechanics.

2.6.2 Relationship between *K* and Global Behavior

In order for the stress intensity factor to be useful, one must be able to determine K from remote loads and the geometry. Closed-form solutions for K have been derived for a number of simple configurations. For more complex situations, the stress intensity factor can be estimated by experiment or numerical analysis (see Chapter 12).

One configuration for which a closed-form solution exists is a through crack in an infinite plate subjected to remote tensile stress (Figure 2.3). Since the remote stress, σ, is perpendicular to the crack plane, the loading is pure Mode I. Linear elastic bodies must undergo proportional stressing; that is, all stress components at all locations increase in proportion to the remotely applied forces. Thus, the crack tip stresses must be proportional to the remote stress, and K_I is proportional to σ. According to Equations 2.42 through 2.44, stress intensity has units of stress $\sqrt{\text{length}}$. Since the only relevant length scale in Figure 2.3 is the crack size, the relationship between K_I and the global conditions must have the following form:

$$K_I = O\left(\sigma\sqrt{a}\right) \tag{2.47}$$

The actual solution, which is derived in Appendix 2A.3, is given by

$$K_I = \sigma\sqrt{\pi a} \tag{2.48}$$

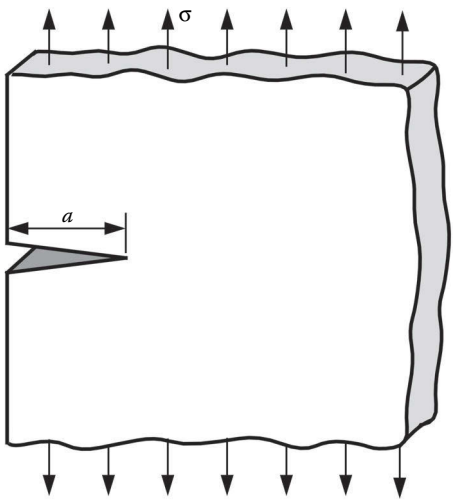

FIGURE 2.16
Edge crack in a semi-infinite plate subject to a remote tensile stress.

Thus, the amplitude of the crack tip singularity for this configuration is proportional to the remote stress and the square root of crack size. The stress intensity factor for Mode II loading of the plate in Figure 2.3 can be obtained by replacing σ in Equation 2.48 by the remotely applied shear stress (see Figure 2.18 and Equations 2.50 and 2.51).

A related solution is that for a semi-infinite plate with an edge crack (Figure 2.16). Note that this configuration can be obtained by slicing the plate in Figure 2.3 through the middle of the crack. The stress intensity factor for the edge crack is given by

$$K_I = 1.12\sigma\sqrt{\pi a} \tag{2.49}$$

which is similar to Equation 2.48. The 12% increase in K_I for the edge crack is caused by different boundary conditions at the free edge. As Figure 2.17 illustrates, the edge crack

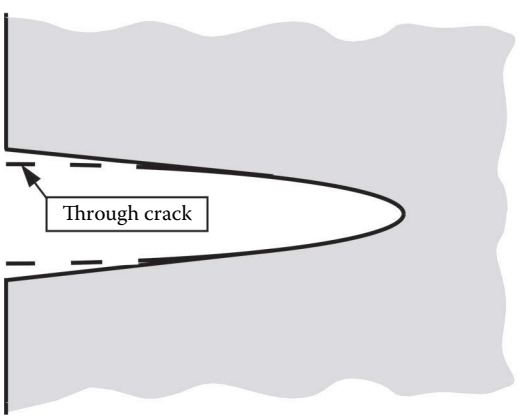

FIGURE 2.17
Comparison of crack opening displacements for an edge crack and through crack. The edge crack opens wider at a given stress, resulting in a stress intensity that is 12% higher.

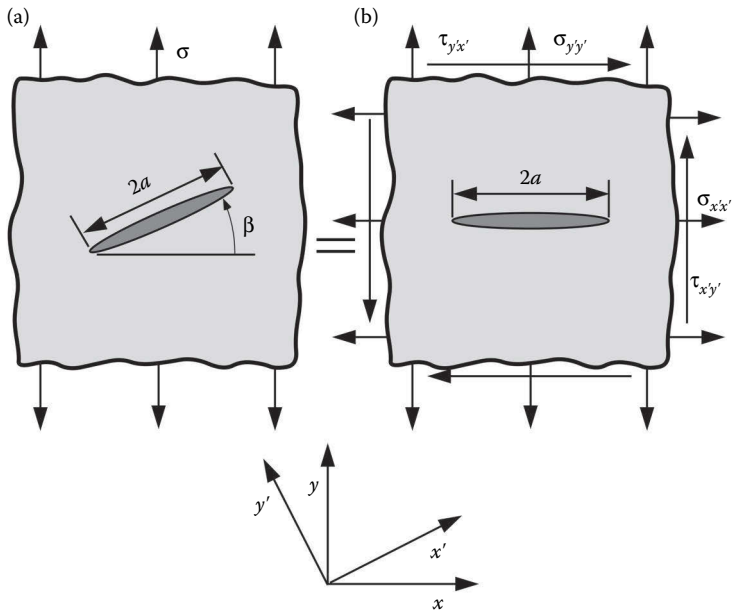

FIGURE 2.18
Through crack in an infinite plate for the general case where the principal stress is not perpendicular to the crack plane.

opens more because it is less restrained than the through crack, which forms an elliptical shape when loaded.

Consider a through crack in an infinite plate where the normal to the crack plane is oriented at an angle β with the stress axis (Figure 2.18a). If $\beta \neq 0$, the crack experiences combined Modes I and II loading; $K_{III} = 0$ as long as the stress axis and the crack normal both lie in the plane of the plate. If we redefine the coordinate axis to coincide with crack orientation (Figure 2.18b), we see that the applied stress can be resolved into normal and shear components. The stress normal to the crack plane, $\sigma_{y'y'}$, produces pure Mode I loading, while $\tau_{x'y'}$ applies Mode II loading to the crack. The stress intensity factors for the plate in Figure 2.18 can be inferred by relating $\sigma_{y'y'}$ and $\tau_{x'y'}$ to σ and β through Mohr's circle:

$$\begin{aligned} K_I &= \sigma_{y'y'}\sqrt{\pi a} \\ &= \sigma \cos^2(\beta)\sqrt{\pi a} \end{aligned} \tag{2.50}$$

and

$$\begin{aligned} K_{II} &= \tau_{x'y'}\sqrt{\pi a} \\ &= \sigma \sin(\beta)\cos(\beta)\sqrt{\pi a} \end{aligned} \tag{2.51}$$

Note that Equations 2.50 and 2.51 reduce to pure Mode I solution when $\beta = 0$. The maximum K_{II} occurs at $\beta = 45°$, where the shear stress is also at a maximum. Section 2.11 addresses fracture under mixed-mode conditions.

The penny-shaped crack in an infinite medium (Figure 2.4) is another configuration for which a closed-form K_I solution exists [11]:

$$K_I = \frac{2}{\pi}\sigma\sqrt{\pi a} \tag{2.52}$$

where a is the crack radius. Note that Equation 2.52 has the same form as the previous relationships for a through crack, except that the crack radius is the characteristic length in the above equation. The more general case of an elliptical or semi-elliptical flaw is illustrated in Figure 2.19. In this instance, two length dimensions are needed to characterize the crack size: $2c$ and $2a$, the major and minor axes of the ellipse, respectively (see Figure 2.19). Moreover, when $a < c$, the stress intensity factor varies along the crack front, with the maximum K_I at $\phi = 90°$. The flaw shape parameter, Q, is obtained from an elliptic integral, as discussed in Appendix 2A.4. Figure 2.19 gives an approximate solution for Q. The surface correction factor, λ_s, is also an approximation.

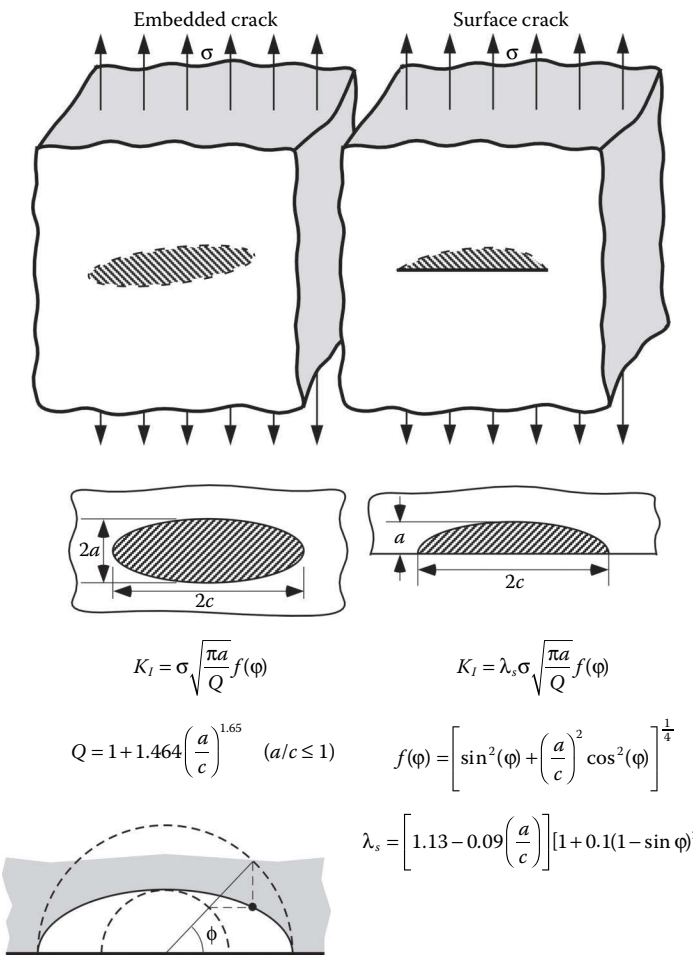

FIGURE 2.19
Mode I stress intensity factors for elliptical and semi-elliptical cracks. These solutions are valid only as long as the crack is small compared with the plate dimensions and $a \le c$.

2.6.3 Effect of Finite Size

Most configurations for which there is a closed-form K solution consist of a crack with a simple shape (e.g., a rectangle or ellipse) in an infinite plate. Stated another way, the crack dimensions are small compared with the size of the plate; the crack tip conditions are not influenced by external boundaries. As the crack size increases, or as the plate dimensions decrease, the outer boundaries begin to exert an influence on the crack tip. In such cases, a closed-form stress intensity solution is usually not possible.

Consider a cracked plate subjected to remote tensile stress. Figure 2.20 schematically illustrates the effect of finite width on the crack tip stress distribution, which is represented by lines of force; the local stress is proportional to the spacing between lines of force. Since a tensile stress cannot be transmitted through a crack, the lines of force are diverted around the crack, resulting in a local stress concentration. In the infinite plate, the line of force at a distance W from the crack centerline has force components in x and y directions. If the plate width is restricted to $2W$, the x force must be zero on the free edge; this boundary condition causes the lines of force to be compressed, which results in higher stress intensification at the crack tip.

One technique to approximate the finite width boundary condition is to assume a periodic array of collinear cracks in an infinite plate (Figure 2.21). The Mode I stress intensity factor for this situation is given by

$$K_I = \sigma\sqrt{\pi a}\left[\frac{2W}{\pi a}\tan\left(\frac{\pi a}{2W}\right)\right]^{1/2} \tag{2.53}$$

The stress intensity approaches the infinite plate value as a/W approaches zero; K_I is asymptotic to $a/W = 1$.

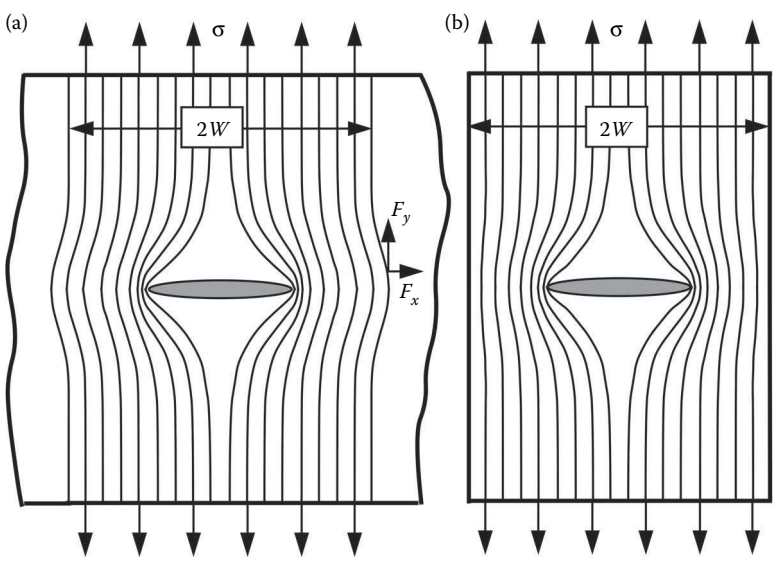

FIGURE 2.20
Stress concentration effects due to a through crack in finite and infinite width plates: (a) infinite plate and (b) finite plate.

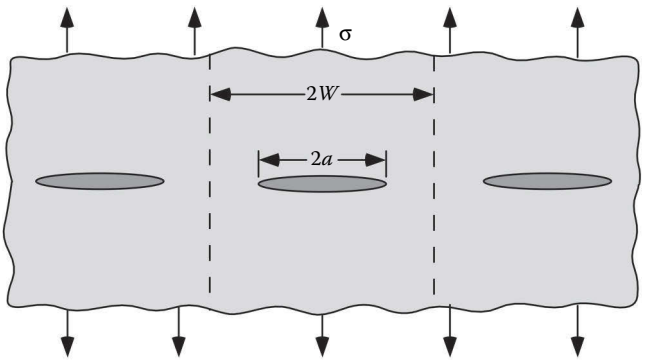

FIGURE 2.21
Collinear cracks in an infinite plate subjected to remote tension.

More accurate solutions for a through crack in a finite plate have been obtained from finite element analysis; solutions of this type are usually fit to a polynomial expression. One such solution [12] is given by

$$K_I = \sigma\sqrt{\pi a}\left[\sec\left(\frac{\pi a}{2W}\right)^{1/2}\right]\left[1-0.025\left(\frac{a}{W}\right)^2+0.06\left(\frac{a}{w}\right)^4\right] \tag{2.54}$$

Figure 2.22 compares the finite-width corrections in Equations 2.53 and 2.54. The secant term (without the polynomial term) in Equation 2.54 is also plotted. Equation 2.53 agrees with the finite element solution to within 7% for $a/W < 0.6$. The secant correction is much closer to the finite element solution; the error is less than 2% for $a/W < 0.9$. Thus, the polynomial term in Equation 2.54 contributes little and can be neglected in hand calculations.

Table 2.4 lists the stress intensity solutions for several common configurations. These K_I solutions are plotted in Figure 2.23. Several handbooks devoted solely to stress intensity solutions have been published [12–14].

Although stress intensity solutions are given in a variety of forms, K can always be related to the through crack (Figure 2.4) through an appropriate correction factor:

$$K_{(I,II,III)} = Y\sigma\sqrt{\pi a} \tag{2.55}$$

where σ is a characteristic stress, a the characteristic crack dimension, and Y is a dimensionless constant that depends on geometry and mode of loading.

EXAMPLE 2.4

Show that the K_I solution for the single-edge notched tensile panel reduces to Equation 2.49 when $a \ll W$.

Solution

All of the K_I expressions in Table 2.4 are of the form

$$K_I = \frac{P}{B\sqrt{W}} f\left(\frac{a}{w}\right)$$

where P is the applied force, B the plate thickness, and $f(a/W)$ is a dimensionless function. The above equation can be expressed in the form of Equation 2.55:

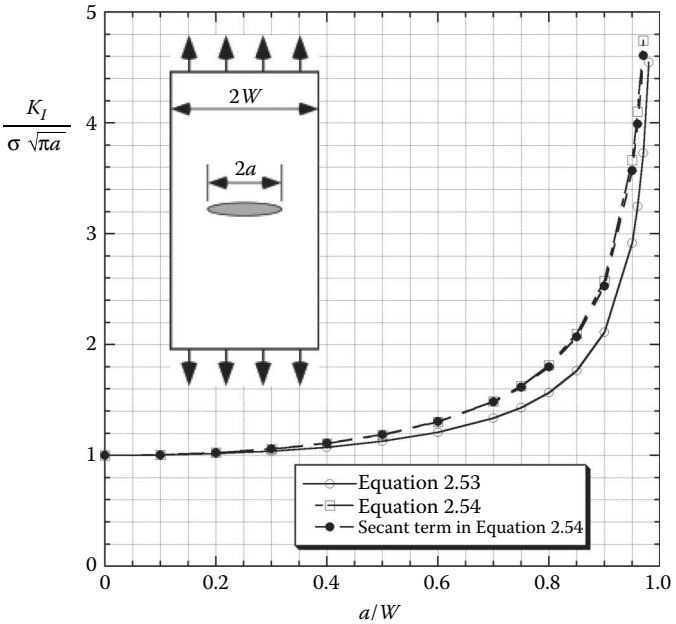

FIGURE 2.22
Comparison of finite-width corrections for a center-cracked plate in tension.

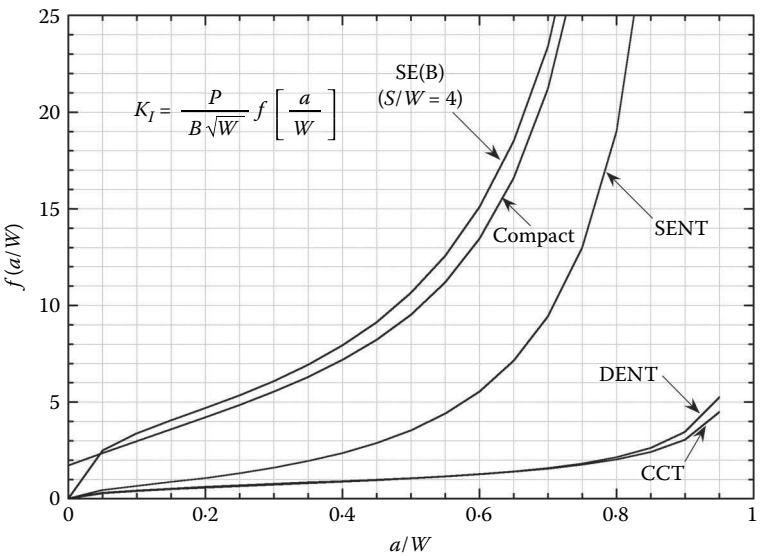

FIGURE 2.23
Plot of stress intensity solutions from Table 2.4.

TABLE 2.4

KI Solutions for Common Test Specimens

Geometry	$f\left(\frac{a}{W}\right)^{a}$
Single-edge notched tension (SENT) 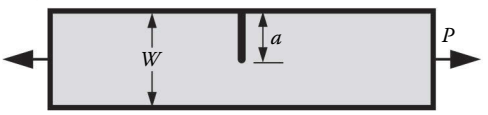	$\frac{\sqrt{2\tan(\pi a/2W)}}{\cos(\pi a/2W)}\left[0.752+2.02\left(\frac{a}{W}\right)+0.37\left(1-\sin\frac{\pi a}{2W}\right)^{3}\right]$
Single-edge notched bend (SE(B)) 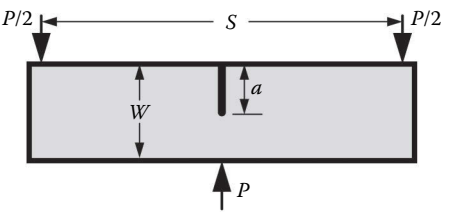	$\frac{3(S/W)\sqrt{a/W}}{2(1+2(a/W))(1-(a/W))^{3/2}}\left[1.99-\frac{a}{W}\left(1-\frac{a}{W}\right)\left\{2.15-3.93\left(\frac{a}{W}\right)+2.7\left(\frac{a}{W}\right)^{2}\right\}\right]$
Center-cracked tension (CCT) 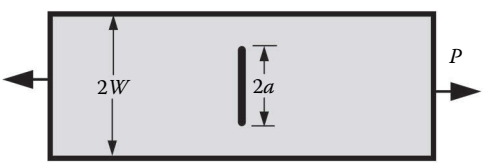	$\sqrt{\frac{\pi a}{4W}\sec\left(\frac{\pi a}{2W}\right)}\left[1-0.025\left(\frac{a}{W}\right)^{2}+0.06\left(\frac{a}{W}\right)^{4}\right]$
Double-edge notched tension (DENT) 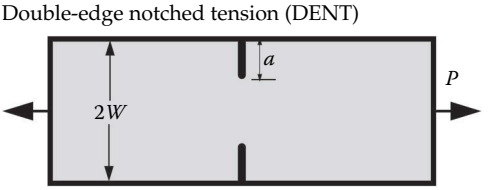	$\frac{\sqrt{\pi a/2W}}{\sqrt{1-(a/W)}}\left[1.122-0.561\left(\frac{a}{W}\right)-0.205\left(\frac{a}{W}\right)^{2}+0.471\left(\frac{a}{W}\right)^{3}+0.190\left(\frac{a}{W}\right)^{4}\right]$
Compact specimen 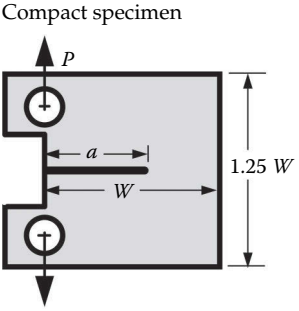	$\frac{2+(a/W)}{(1-(a/W))^{3/2}}\left[0.886+4.64\left(\frac{a}{W}\right)-13.32\left(\frac{a}{W}\right)^{2}+14.72\left(\frac{a}{W}\right)^{3}-5.60\left(\frac{a}{W}\right)^{4}\right]$

Source: Adapted from Tada, H., Paris, P.C., and Irwin, G.R., *The Stress Analysis of Cracks Handbook* (2nd ed.), Paris Productions, Inc., St. Louis, 1985.

[a] $K_I = \frac{P}{B\sqrt{W}} f\left(\frac{a}{W}\right)$, where B is the specimen thickness.

$$\frac{P}{B\sqrt{W}} f\left(\frac{a}{w}\right) = \frac{P}{BW} f\left(\frac{a}{w}\right)\sqrt{\frac{W}{\pi a}}\sqrt{\pi a} = Y\sigma\sqrt{\pi a}$$

where

$$Y = f\left(\frac{a}{W}\right)\sqrt{\frac{W}{\pi a}}$$

In the limit of a small flaw, the geometry correction factor in Table 2.4 becomes

$$\lim_{a/W\to 0} f\left(\frac{a}{W}\right) = \sqrt{\frac{\pi a}{W}}[0.752 + 0.37]$$

Thus,

$$\lim_{a/W\to 0} Y = 1.122$$

2.6.4 Principle of Superposition

For linear elastic materials, individual components of stress, strain, and displacement are additive. For example, two normal stresses in the x direction imposed by different external forces can be added to obtain the total σ_{xx}, but a normal stress cannot be summed with a shear stress. Similarly, stress intensity factors are additive as long as the mode of loading is consistent. That is,

$$K_I^{(\text{total})} = K_I^{(A)} + K_I^{(B)} + K_I^{(C)}$$

but

$$K_{(\text{total})} \neq K_I + K_{II} + K_{III}$$

In many instances, the principle of superposition allows stress intensity solutions for complex configurations to be built from simple cases for which the solutions are well established. Consider, for example, an edge-cracked panel (Table 2.4) subject to combined membrane (axial) loading, P_m, and three-point bending, P_b. Since both types of loading impose pure Mode I conditions, the K_I values can be added:

$$\begin{aligned} K_I^{(\text{total})} &= K_I^{(\text{membrane})} + K_I^{(\text{bending})} \\ &= \frac{1}{B\sqrt{W}}\left[P_m f_m\left(\frac{a}{W}\right) + P_b f_b\left(\frac{a}{W}\right)\right] \end{aligned} \tag{2.56}$$

where f_m and f_b are the geometry correction factors for membrane and bending loading, respectively, listed in Table 2.4 and plotted in Figure 2.23.

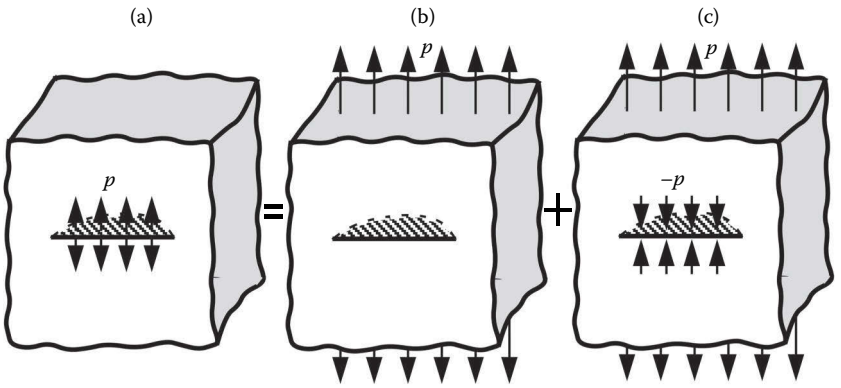

FIGURE 2.24
Determination of K_I for a semi-elliptical surface crack under internal pressure, p, by means of the principle of superposition.

EXAMPLE 2.5

Determine the stress intensity factor for a semi-elliptical surface crack subjected to an internal pressure, p (Figure 2.24a).

Solution

The principle of superposition enables us to construct the solution from known cases. One relevant case is the semi-elliptical surface flaw under uniform remote tension, p (Figure 2.24b). If we impose a uniform compressive stress, $-p$, on the crack surface (Figure 2.24c), $K_I = 0$ because the crack faces close and the plate behaves as if the crack were not present. The loading configuration of interest is obtained by subtracting the stresses in Figure 2.24c from those of Figure 2.24b:

$$K_I^{(a)} = K_I^{(b)} - K_I^{(c)}$$
$$= \lambda_s p\sqrt{\frac{\pi a}{Q}} f(\phi) - 0 = \lambda_s p\sqrt{\frac{\pi a}{Q}} f(\phi)$$

Example 2.5 is a simple illustration of a more general concept: namely, stresses acting on the boundary (i.e., tractions) can be replaced with tractions that act on the crack face, such that the two loading configurations (boundary tractions vs. crack face tractions) result in the same stress intensity factor. Consider an uncracked body subject to a boundary traction $P(x)$, as illustrated in Figure 2.25. This boundary traction results in a normal stress distribution $p(x)$ on Plane A–B. To confine the problem to Mode I, let us assume that no shear stresses act on Plane A–B. (This assumption is made only for the sake of simplicity; the basic principle can be applied to all three modes of loading.) Now assume that a crack that forms on Plane A–B and the boundary traction, $P(x)$, remains fixed, as Figure 2.26a illustrates. If we remove the boundary traction and apply a traction $p(x)$ on the crack face (Figure 2.26b), the principle of superposition indicates that the applied K_I will be unchanged. That is,

$$K_I^{(a)} = K_I^{(b)} + K_I^{(c)} = K_I^{(b)} \quad (\text{since } K_I^{(c)} = 0)$$

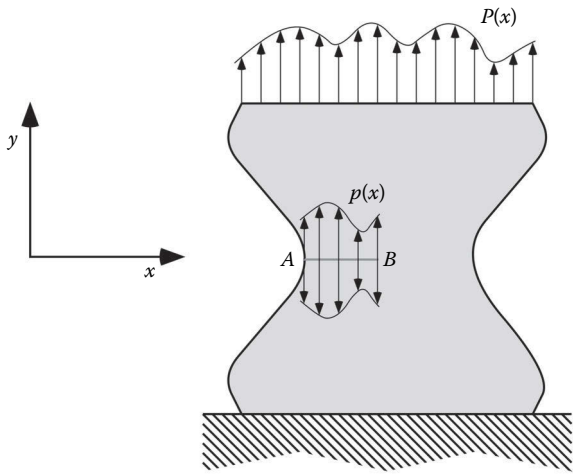

FIGURE 2.25
Uncracked body subjected to an arbitrary boundary traction $P(x)$, which results in a normal stress distribution $p(x)$ acting on Plane A–B.

2.6.5 Weight Functions

When one performs an analysis to infer a stress intensity factor for a cracked body, the K value that is computed applies only to one particular set of boundary conditions; different load cases result in different stress intensity factors for that geometry. It turns out, however, that the solution to one set of boundary conditions contains sufficient information to infer K for *any other* boundary conditions on that same geometry.

Consider two arbitrary loading conditions on an isotropic elastic cracked body in plane stress or plane strain. For now, we assume that both loadings are symmetric with respect to the crack plane, such that pure Mode I loading is achieved in each case. Suppose that we know the stress intensity factor for loading (1) and we wish to solve for $K_I^{(2)}$, the stress

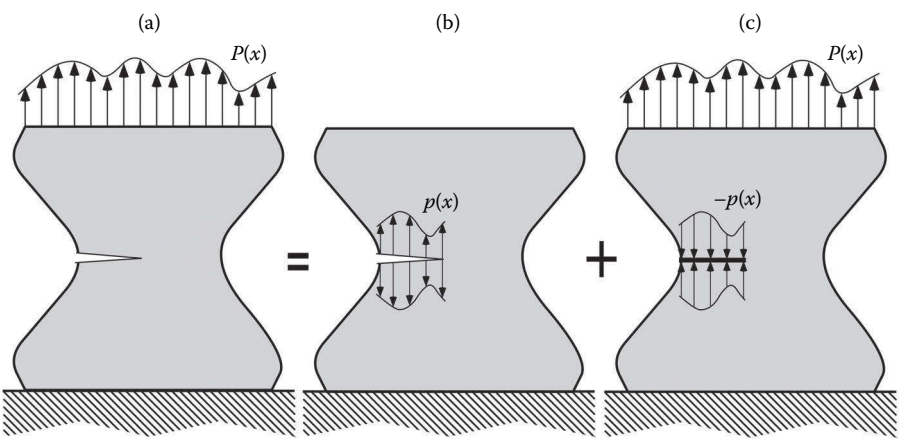

FIGURE 2.26
Application of superposition to replace a boundary traction $P(x)$ with a crack face traction $p(x)$ that results in the same K_I.

intensity factor for the second set of boundary conditions. Rice [15] has shown that $K_I^{(1)}$ and $K_I^{(2)}$ are related as follows:

$$K_I^{(2)} = \frac{E'}{2K_I^{(1)}}\left[\int_\Gamma T_i \frac{\partial u_i^{(1)}}{\partial a} d\Gamma + \int_A F_i \frac{\partial u_i^{(1)}}{\partial a} dA\right] \tag{2.57}$$

where Γ and A are the perimeter and area of the body, respectively, and u_i are the displacements in x and y directions. Since loading systems (1) and (2) are arbitrary, it follows that $K_I^{(2)}$ cannot depend on $K_I^{(1)}$ and $u_i^{(1)}$. Therefore, the function

$$h(x_i) = \frac{E}{2K_I^{(1)}} \frac{\partial u_i^{(1)}}{\partial a} \tag{2.58}$$

where x_i represents the x and y coordinates, must be independent of the nature of loading system (1). Bueckner [16] derived a result similar to Equation 2.58 two years before Rice, and referred to h as a *weight function*.

Weight functions are first-order tensors that depend only on the geometry of the cracked body. Given the weight function for a particular configuration, it is possible to compute K_I from Equation 2.57 for any boundary conditions. Moreover, the previous section invoked the principle of superposition to show that any loading configuration can be represented by appropriate tractions applied directly to the crack face. Thus, K_I for a 2D cracked body can be inferred from the following expression:

$$K_I = \int_{\Gamma_c} p(x)h(x)\,dx \tag{2.59}$$

where $p(x)$ is the crack face traction (equal to the normal stress acting on the crack plane when the body is uncracked) and Γ_c is the perimeter of the crack. The weight function, $h(x)$, can be interpreted as the stress intensity resulting from a unit force applied to the crack face at x, and the above integral represents the superposition of the K_I values from discrete opening forces along the crack face.

EXAMPLE 2.6

Derive an expression for K_I for an arbitrary traction on the face of a through crack in an infinite plate.

Solution

We already know K_I for this configuration when a uniform tensile stress is applied:

$$K_I = \sigma\sqrt{\pi a}$$

where a is the half crack length. From Equation 2A.74 and 2A.75, the opening displacement of the crack faces in this case is given by

$$u_y = \pm\frac{2\sigma}{E'}\sqrt{x(2a-x)}$$

where the x–y coordinate axis is defined in Figure 2.27a. Since the crack length is $2a$, we must differentiate u_y with respect to $2a$ rather than a:

$$\frac{\partial u_y}{\partial(2a)} = \pm\frac{2\sigma}{E}\sqrt{\frac{x}{2a-x}}$$

Thus, the weight function for this crack geometry is given by

$$h(x) = \pm\frac{1}{\sqrt{\pi a}}\sqrt{\frac{x}{2a-x}}$$

If we apply a surface traction of $\pm p(x)$ on the crack faces, the Mode I stress intensity factor for the two crack tips is as follows:

$$K_{I(x=2a)} = \frac{1}{\sqrt{\pi a}}\int_0^{2a} p(x)\sqrt{\frac{x}{2a-x}}\,dx$$

$$K_{I(x=0)} = \frac{1}{\sqrt{\pi a}}\int_0^{2a} p(x)\sqrt{\frac{2a-x}{x}}\,dx$$

The weight function concept is not restricted to 2D bodies, Mode I loading, or isotropic elastic materials. In their early work on weight functions, Rice [15] extended the theory to three dimensions, Bueckner [16] considered combined Mode I/II loading, and both allowed for anisotropy in the elastic properties. Subsequent researchers [17–22] have shown that the theory applies to all linear elastic bodies that contain an arbitrary number of cracks.

For mixed-mode problems, separate weight functions are required for each mode: h_I, h_{II}, and h_{III}. Since the stress intensity factors can vary along a 3D crack front, the weight functions also vary along the crack front. That is,

$$h_a = h_a(x_i, \eta) \tag{2.60}$$

where α(=1,2,3) indicates the mode of loading and η is the crack front position.

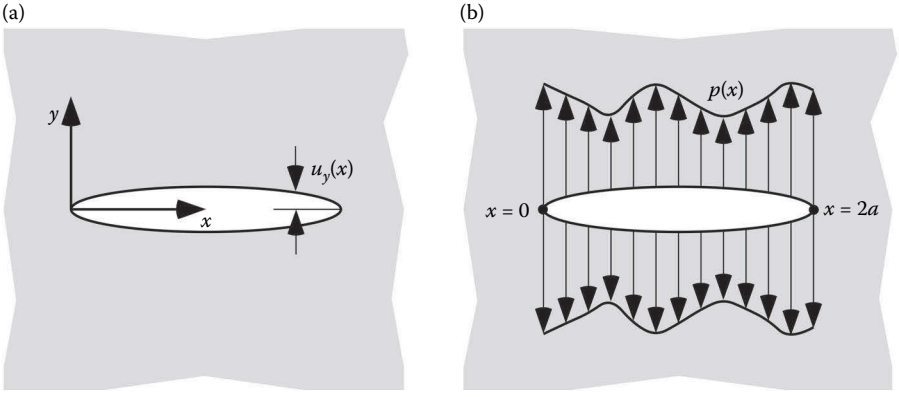

FIGURE 2.27
Through-crack configuration analyzed in Example 2.6: (a) Definition of coordinate axes and (b) arbitrary traction applied to crack faces.